

# Ferrocenoyl Amino Acids: A Synthetic and Structural Study<sup>†</sup>

Heinz-Bernhard Kraatz,\* Janusz Luszyk, and Gary D. Enright

Chemical Biology Program, Steacie Institute for Molecular Sciences, National Research Council of Canada, 100 Sussex Drive, Ottawa, Ontario K1A 0R6, Canada

Received December 4, 1996<sup>⊗</sup>

A series of ester-protected amino acids were coupled to ferrocenecarboxylic acid (**1**) using the DCC/HOBt protocol to give ferrocenoyl *N*-amino acids (amino acid = Glu(OBz)<sub>2</sub> (**2a**), Gly(OEt) (**2b**), Pro(OBz) (**2c**), Cys(SBz)OMe (**2d**), Ala(OBz) (**2e**), Tyr(OBz) (**2f**), Phe(OBz) (**2g**)). All products were fully characterized. The intermediate hydroxybenzotriazole active ester FcCOOBt (**3**) was isolated and fully characterized. The solid state structures of **2a**, **2d**, and **3** were determined by single-crystal X-ray diffraction. **2a**: monoclinic *P*2<sub>1</sub> with *a* = 11.8142(5) Å, *b* = 9.7560(5) Å, *c* = 22.9456(10) Å, β = 90.246(5)°, *V* = 2644.7(2) Å<sup>3</sup>, *Z* = 2, *R* = 0.046. **2d**: orthorhombic *P*2<sub>1</sub>2<sub>1</sub>2<sub>1</sub> with *a* = 9.957(2) Å, *b* = 11.680(2) Å, *c* = 36.452(2) Å, *V* = 4239.5(13) Å<sup>3</sup>, *Z* = 4, *R* = 0.065. The solid state structures of **2a** and **2d** show extensive C=O···H–N hydrogen bonding. **3**: triclinic *P*1 with *a* = 7.0391(5) Å, *b* = 10.7922(7) Å, *c* = 11.1690(7) Å, α = 108.071(5)°, β = 107.957(5)°, γ = 103.896(5)°, *V* = 712.5(2) Å<sup>3</sup>, *Z* = 2, *R* = 0.030. The long ester bond distance of 1.427(2) Å provides a rationale for its inherent reactivity toward primary and secondary amines.

## Introduction

A transition metal can be intimately involved in electron transfer (ET) processes either as an electron storage device, as part of an electron transfer chain, or as the reaction center itself.<sup>1</sup> Progress has been made in understanding ET processes by making use of chemically modified metalloproteins,<sup>2</sup> which has provided much insight into the redox behavior of the active site. It is generally believed that long range ET occurs by tunneling, while short-range ET may proceed by a through-bond mechanism. The particular redox characteristics of a metal center are likely to depend most critically on (a) small deviations from the standard geometry imposed on the metal center by the protein backbone, (b) the extended chemical environment imposed on the metal by the tertiary structure of the protein, and (c) direct metal–protein interactions. The influence of the protein backbone on the stabilization of one redox state of a metal over another has been implied. However, the role of the protein backbone in modifying ET rates and its mechanisms is only poorly understood. ET rate measurements for systems having two redox centers linked by a linear peptide chain have appeared in the literature over the years.<sup>3</sup> It was shown generally that a high flexibility of the oligopeptide linker results

in a lower observed rate.<sup>3a–e</sup> Furthermore, it was recognized that the rate is influenced by the electric field generated in helical peptide assemblies, and hence by the direction of ET.<sup>3p</sup>

We are interested in the ET properties of rigid and flexible peptide assemblies, addressing the role of the peptidic backbone in ET processes. As part of our ongoing investigation, we hope to be able to delineate through-bond and through-space interactions and draw conclusions about electronic effects of each amino acid residue. However, in order to draw meaningful conclusions about electronic properties of a particular system, structural and theoretical considerations must be taken into account. In addition, it has been widely recognized that the dynamic properties of the system are an important factor in the electron transfer process. The size of natural systems precludes a detailed investigation of structural reorganization processes that may occur during ET.

Rather than having to cope with large redox proteins, we are focusing our attention on small peptide assemblies covalently linked to various redox probes. These systems can be structurally characterized by NMR methods and X-ray crystallography. In addition, their size does not preclude high-level calculations (e.g., density functional calculations). In our approach, the redox probe is coupled to an amino acid and/or peptides of defined chain length and structure. Ferrocene moieties have been widely used in molecular recognition studies as probe molecules, sensitive to small changes in electronic structure brought about by substrate binding.<sup>4</sup> Binding is achieved by

\* Corresponding author. E-mail: bernie@100sci.lan.nrc.ca.

<sup>†</sup> Issued as NRCC-39137.

<sup>⊗</sup> Abstract published in *Advance ACS Abstracts*, April 1, 1997.

- (1) Bertini, I.; Gray, H. B.; Lippard, S. J.; Valentine, J. S. *Bioinorganic Chemistry*. University Science Books: Mill Valley, CA, 1994.
- (2) (a) Meier, M.; van Eldik, R.; Chang, I.-L.; Mines, G. A.; Wuttke, D. S.; Winkler, J. R.; Gray, H. B. *J. Am. Chem. Soc.* **1994**, *116*, 1577–1578. (b) Wuttke, D. S.; Gray, H. B.; Fisher, S. L.; Imperiali, B. *J. Am. Chem. Soc.* **1993**, *115*, 8455–8456. (c) Chang, I.-J.; Gray, H. B.; Winkler, J. R. *J. Am. Chem. Soc.* **1991**, *113*, 7056. (d) Wuttke, D. S.; Bjerrum, M. J.; Winkler, J. R.; Gray, H. B. *Science* **1992**, *256*, 1007.
- (3) (a) Isied, S. S.; Vassilin, A. *J. Am. Chem. Soc.* **1984**, *106*, 1726–1732. (b) Isied, S. S.; Vassilin, A. *J. Am. Chem. Soc.* **1984**, *106*, 1736–1739. (c) Isied, S. S.; Vassilin, A.; Magnuson, R. H.; Schwarz, H. A. *J. Am. Chem. Soc.* **1985**, *107*, 7432–7438. (d) Vassilin, A.; Wishart, J. F.; van Hemelryck, B.; Schwarz, H. A.; Isied, S. S. *J. Am. Chem. Soc.* **1990**, *112*, 7258–7266. (e) For a review see: Isied, S. S. *Chem. Rev.* **1992**, *92*, 381. (f) Schanze, K. S.; Sauer, K. J. *J. Am. Chem. Soc.* **1988**, *110*, 1180–1186. (g) Sisido, M.; Tanaka, R.; Inai, Y.; Imanishi, Y. *J. Am. Chem. Soc.* **1989**, *111*, 6790–6796. (h) Farraggi, M.; DeFilippis, M. R.; Klapper, M. H. *J. Am. Chem. Soc.* **1989**, *111*, 5141–5145. (i) DeFilippis, M. R.; Farraggi, M.; Klapper, M. H. *J.*

*Am. Chem. Soc.* **1990**, *112*, 5640–5642. (j) Basu, G.; Kubasik, M.; Angelos, D.; Secor, B.; Kuki, A. *J. Am. Chem. Soc.* **1990**, *112*, 9410–9411. (k) Mecklenburg, S. L.; Peek, B. M.; Erickson, B. W.; Meyer, T. J. *J. Am. Chem. Soc.* **1991**, *113*, 8540–8542. (l) Mecklenburg, S. L.; Peek, B. M.; Schoonover, J. R.; McCafferty, D. G.; Wall, C. G.; Erickson, B. W.; Meyer, T. J. *J. Am. Chem. Soc.* **1993**, *115*, 5479–5495. (m) Mishna, A. K.; Chandrasekar, R.; Faraggi, M.; Klapper, M. H. *J. Am. Chem. Soc.* **1994**, *116*, 1414–1422. (n) Hayashi, T.; Takimura, T.; Hitomi, Y.; Ohara, T.; Ogoshi, H. *J. Chem. Soc. Chem. Commun.* **1995**, 545–555. (o) Jones, G.; Feng, Z.; Oh, C. *J. Phys. Chem.* **1995**, *99*, 3883–3888. (p) Galoppini, E.; Fox, M. A. *J. Am. Chem. Soc.* **1996**, *118*, 2299–2300.

- (4) (a) For a recent survey see: Beer, P. D. *J. Chem. Soc., Chem. Commun.* **1996**, 689–696. (b) Chen, Z.; Graydon, A. R.; Beer, P. D. *J. Chem. Soc., Faraday Trans.* **1996**, *92*, 97–102. (c) Also see: Constable, E. C. *Angew. Chem., Int. Ed. Engl.* **1991**, *30*, 407–408.

simple coupling reactions, such as esterification or amidation.<sup>5a-c</sup> Other methods include the introduction of the ferrocenylmethyl (Fem) group by catalytic reductive alkylation of amino acids<sup>5d,e</sup> and the Pd-catalyzed coupling of iodoferrocenes with 2-amidoacrylates.<sup>5f</sup> Degani and Heller have coupled the ferrocene moiety to glucose oxidase via the H<sub>2</sub>N group of lysine and used it as a redox relay.<sup>6</sup> Coupling was achieved using a water-soluble carbodiimide (1-(3-(dimethylamino)propyl)-3-ethylcarbodiimide). There is no structural information about the ferrocene-protein linkage and its arrangement with respect to the rest of the protein.

We now wish to report our first study focusing on synthetic results of ferrocenecarboxylic acid/amino acid coupling reactions. The structural properties of two ferrocenyl-amino acid esters and of ferrocenylhydroxybenzotriazole active ester are described. A preliminary account of this work was presented earlier.<sup>7</sup>

## Experimental Section

**General Procedures.** Glutamic acid dibenzyl ester was prepared according to the published procedure from L-glutamic acid (Aldrich) and benzyl alcohol under acidic conditions.<sup>8</sup> H-Gly(OEt)·HCl, H-Pro(OBz)·HCl, H-Cys(SBz)OMe·HCl, ferrocenecarboxylic acid (FC), dicyclohexylcarbodiimide (DCC), and Hydroxybenzotriazole (HOBT) were used as received (Aldrich). H-Ala(OBz)·Tos and H-Tyr(OBz)·Tos (Nova-Biochem) were used as received. All solvents were used as received without further treatment. <sup>1</sup>H- and <sup>13</sup>C-NMR spectra were recorded at 200.132 and 50.323 MHz, respectively, on a Bruker AC 200 NMR spectrometer. 2D-COSY spectra were recorded at 500.14 MHz on a Bruker AMX 500 NMR spectrometer. All chemical shifts ( $\delta$ ) are reported in ppm and coupling constants ( $J$ ) in Hz. The <sup>1</sup>H- and <sup>13</sup>C-NMR chemical shifts are relative to tetramethylsilane ( $\delta = 0$  ppm), which was added as an internal standard. Assignments in the <sup>1</sup>H- and <sup>13</sup>C{<sup>1</sup>H}-NMR were made using <sup>13</sup>C-DEPT-135 (distortionless enhancement by polarization transfer) and by 2D-COSY. All measurements were carried out at 293 K unless otherwise specified. Elemental analyses were carried out at the NRC Institute for Biology, Ottawa, Canada.

**Preparation of Ferrocenyl Amino Acids. Ferrocenyl-N-Glutamic Acid Dibenzyl Ester (2a).** To a solution of ferrocenecarboxylic acid (0.55 g, 2.4 mmol) in CH<sub>2</sub>Cl<sub>2</sub> (10 mL) were added solid dicyclohexylcarbodiimide (0.50 g, 2.4 mmol) and HOBT (0.34 g, 2.4 mmol). Freshly prepared glutamic acid dibenzyl ester hydrochloric acid salt (1.57 g, 4.8 mmol) was treated with Et<sub>3</sub>N in CH<sub>2</sub>Cl<sub>2</sub>, and the mixture was added to the stirring slurry. Dicyclohexylurea precipitated almost immediately. Stirring was continued at room temperature for 2 days. The urea was filtered off, and the filtrate was washed with distilled water (3 × 100 mL) and subsequently dried over MgSO<sub>4</sub>. The solvent was removed in vacuo. The crude product (0.81 g, 62.7%) was recrystallized from ethyl acetate and then from diethyl ether to give 0.45 g of yellow needles (yield 34.6%), which were of sufficient quality to be used in the X-ray crystallographic study. Anal. Calc for

C<sub>30</sub>H<sub>29</sub>FeNO<sub>5</sub>: C, 66.80; H, 5.42; N, 2.60. Found: C, 67.1; H, 5.6; N, 3.0. MW for C<sub>30</sub>H<sub>29</sub>FeNO<sub>5</sub>: calc, 539.4; found, 540.2 [M + 1]<sup>+</sup>.  $E_{1/2} = 0.180$  V (vs Fc/Fc<sup>+</sup>). IR (film; cm<sup>-1</sup>; NaCl plates): 3400 ( $\nu$ (N-H), vbr), 1734 (br) and 1627 ( $\nu$ (C=O)). <sup>1</sup>H-NMR ( $\delta$  in ppm, CDCl<sub>3</sub>): 7.36–7.25 (m, aromatic H of Ph), 6.63 (1H, br d,  $J_{\text{HH}} = 7.7$  Hz, -NH), 5.21 (2H, s, PhCH<sub>2</sub>O), 5.10 (2H, s, PhCH<sub>2</sub>O), 4.77 (2H, m, -NCH- and H ortho to carboxy group on Cp ring, both signals overlapping), 4.64 (1H, s, H ortho to carboxy group on Cp ring), 4.34 (2H, br s, H meta to carboxy group on Cp ring), 4.21 (5H, s, unsubstituted Cp ring), 2.49 (2H, m, -CH<sub>2</sub>CH<sub>2</sub>COOBz), 2.35 (2H, m, -CH<sub>2</sub>CH<sub>2</sub>COOBz). <sup>13</sup>C-NMR ( $\delta$  in ppm, CDCl<sub>3</sub>): 173.2 (C=O), 171.9 (C=O), 170.6 (C=O), 135.6 (quaternary C of Ph), 135.2 (+ve DEPT, Ph), 128.6 (+ve DEPT, Ph), 128.4 (+ve DEPT, Ph), 128.3 (+ve DEPT, Ph), 74.9 (quaternary C of Cp), 70.6 (+ve DEPT, 2C meta to carboxy group on Cp ring), 69.7 (+ve DEPT, all C of unsubstituted Cp), 68.5 (+ve DEPT, C ortho to carboxy group on Cp ring), 67.8 (C ortho to carboxy group on Cp ring), 67.3 (-ve DEPT, -OCH<sub>2</sub>Ph), 66.6 (-ve DEPT, -OCH<sub>2</sub>Ph), 51.8 (+ve DEPT, N(H)CH(R)C(O)), 30.4 (-ve DEPT, -CH<sub>2</sub>CH<sub>2</sub>), 26.9 (-ve DEPT, -CH<sub>2</sub>CH<sub>2</sub>).

**General Preparation for 2b-g.** The synthesis employed for the preparation of 2b-g was identical to that for 2a. Ferrocenecarboxylic acid (0.5 g, 2.17 mmol), solid dicyclohexylcarbodiimide (0.50 g, 2.4 mmol), and HOBT (0.34 g, 2.4 mmol) were allowed to react in CH<sub>2</sub>Cl<sub>2</sub> (10 mL). Amino acid ester hydrochloric acid salt (exact amount: see *vide infra*) was treated with Et<sub>3</sub>N in CH<sub>2</sub>Cl<sub>2</sub>, and the mixture was added to the stirring slurry. Stirring was continued overnight. The procedure for the isolation of the products was identical to that for 2a.

**Ferrocenyl-N-Gly(OEt) (2b).** H-Gly-OEt (0.35 g, 2.5 mmol) was used. Yield: 0.52 g, 76.0%, yellow microcrystalline solid. Anal. Calc for C<sub>15</sub>H<sub>17</sub>NO<sub>3</sub>Fe: C, 57.16; H, 5.44; N, 4.44. Found: C, 56.9; H, 5.5; N, 5.0. MW for C<sub>15</sub>H<sub>17</sub>NO<sub>3</sub>Fe: calc, 315.2; found, 316.1 [M + 1]<sup>+</sup>.  $E_{1/2} = 0.181$  V (vs Fc/Fc<sup>+</sup>). <sup>1</sup>H-NMR ( $\delta$  in ppm, CDCl<sub>3</sub>, 20 °C): 6.22 (1H, br s, -NH), 4.72 (2H, t,  $J_{\text{HH}} = 1.8$  Hz, H ortho to carboxy group on Cp ring), 4.36 (2H, t,  $J_{\text{HH}} = 1.8$  Hz, H meta to carboxy group on Cp ring), 4.28 (5H, s, unsubstituted Cp ring), 4.26 (2H, q,  $J_{\text{HH}} = 7.2$  Hz, -OCH<sub>2</sub>-), 4.15 (d,  $J_{\text{NH}} = 5.4$  Hz, N(H)CH<sub>2</sub>C(O)), 1.36 (3H, t,  $J_{\text{HH}} = 7.2$  Hz, -CH<sub>2</sub>CH<sub>3</sub>). <sup>13</sup>C-NMR ( $\delta$  in ppm, CDCl<sub>3</sub>, 20 °C): 71.26 (s, +ve DEPT, C ortho to carboxy group on Fc), 70.49 (s, +ve DEPT, C meta to carboxy group on Fc), 68.90 (s, +ve DEPT, unsubstituted Cp ring of Fc), 62.17 (s, -ve DEPT, -OCH<sub>2</sub>-CH<sub>3</sub>), 42.01 (s, -ve DEPT, -N(H)CH<sub>2</sub>-), 14.87 (s, +ve DEPT, -OCH<sub>2</sub>CH<sub>3</sub>).

**Ferrocenyl-N-Pro(OBz) (2c).** H-Pro-OBz·HCl (0.60 g, 2.48 mmol) was used. Yield: 0.77 g, 85.0%, brown viscous oil. MW for C<sub>23</sub>H<sub>23</sub>NO<sub>3</sub>Fe: calc, 417.3; found, 418.1 [M + 1]<sup>+</sup>.  $E_{1/2} = 0.160$  V (vs Fc/Fc<sup>+</sup>). <sup>1</sup>H-NMR ( $\delta$  in ppm, CDCl<sub>3</sub>): 7.36 (5H, br m, aromatic H of Ph), 5.21 (2H, second-order m, OCH<sub>2</sub>Ph), 4.86 (1H, s, H ortho to carboxy group on Cp ring), 4.70 (2H, m, overlapping signals due to N(H)CH(R)C(O) and H ortho to carboxy group on Cp ring), 4.36 (2H, s, H meta to carboxy group on Cp ring), 4.24 (5H, s, H of unsubstituted Cp ring), 3.96 and 3.79 (2H, m, two signals due to the two diastereotopic H of -NCH<sub>2</sub>-), 2.21 and 1.99 (2H, m, two signals due to the two diastereotopic H adjacent to stereocenter -C(H)CH<sub>2</sub>CH<sub>2</sub>CH<sub>2</sub>N-, overlapping with signal due to one H of the -NCH<sub>2</sub>CH<sub>2</sub>CH<sub>2</sub>- group), 2.09 and 1.99 (2H, m, two signals due to the two diastereotopic H of -NCH<sub>2</sub>CH<sub>2</sub>CH<sub>2</sub>-). <sup>13</sup>C-NMR ( $\delta$  in ppm, CDCl<sub>3</sub>): 172.2 (C=O), 169.7 (C=O), 135.8 (s, quaternary C of Ph), 128.5 (s, Ph), 128.1 (br s, Ph), 73.4 (s, ipso C of Cp), 70.8 (s, C on Cp), 70.2 (s, C on Cp), 70.0 (s, C on Cp), 69.6 (s, unsubstituted Cp ring of Fc), 66.6 (s, -ve DEPT, OCH<sub>2</sub>Ph), 60.2 (s, +ve DEPT, N(H)CH<sub>2</sub>C(O)), 49.0 (s, -ve DEPT, N(H)CH<sub>2</sub>-), 28.6 (s, -ve DEPT, -CH<sub>2</sub>-), 25.5 (s, -ve DEPT, -CH<sub>2</sub>-).

**Ferrocenyl-N-Cys(SBz)OMe (2d).** H-Cys(SBz)-OMe·HCl (0.74 g, 2.2 mmol) was used. The crude orange-yellow material (yield = 0.75 g, 79.0%) was recrystallized from CH<sub>2</sub>Cl<sub>2</sub> and then from Et<sub>2</sub>O. X-ray-quality crystals were obtained as thin yellow needles by slow evaporation of Et<sub>2</sub>O at -20 °C. Anal. Calc for C<sub>22</sub>H<sub>23</sub>NO<sub>3</sub>SFe: C, 60.43; H, 5.30; N, 3.20. Found: C, 60.2; H, 5.4; N, 4.0. MW for C<sub>22</sub>H<sub>23</sub>NO<sub>3</sub>SFe: calc, 437.3; found, 438.1 [M + 1]<sup>+</sup>.  $E_{1/2} = 0.191$  V (vs Fc/Fc<sup>+</sup>). <sup>1</sup>H-NMR ( $\delta$  in ppm, CDCl<sub>3</sub>): 7.32 (5H, m, aromatic H of SCH<sub>2</sub>Ph), 6.47 (1H, d,  $J_{\text{NH}} = 7.0$  Hz, -NH), 4.94 (1H, m, N(H)-CH(R)C(O)), 4.73 (1H, s, H ortho to carboxy group on Cp ring), 4.69

- (5) (a) See for example: Tecilla, P.; Dixon, R. P.; Slobodkin, G.; Alavi, D. S.; Waldeck, D. H.; Hamilton, A. D. *J. Am. Chem. Soc.* **1990**, *112*, 9408–9410. (b) Medina, J. C.; Gay, I.; Chen, Z.; Echegoyen, I.; Gockel, G. W. *J. Am. Chem. Soc.* **1991**, *113*, 365. (c) Medina, J. C.; Li, C.; Bott, S. G.; Atwood, J. L.; Gockel, G. W. *J. Am. Chem. Soc.* **1991**, *113*, 366. (d) Eckert, H.; Seidel, C. *Angew. Chem., Int. Ed. Engl.* **1986**, *25*, 159–160. (e) Beer, P. D.; Chen, Z.; Drew, M. G. B.; Kingston, J.; Ogden, M.; Spencer, P. *J. Chem. Soc., Chem. Commun.* **1993**, 1046–1048. (f) Carlström, A.-S.; Frejd, T. *J. Org. Chem.* **1990**, *55*, 4175–4180.
- (6) (a) Degani, Y.; Heller, A. *J. Phys. Chem.* **1987**, *91*, 1285–1289. (b) Degani, Y.; Heller, A. *J. Am. Chem. Soc.* **1988**, *110*, 2615–2620. (c) For a review of electrode-bound systems see: Heller, A. *J. Chem. Phys.* **1992**, *96*, 3579–3587.
- (7) Kraatz, H.-B. Paper presented at the 3rd European Bioinorganic (EUROBIC3) conference in Noordwijkerhout, The Netherlands, Aug 4–10, 1996; see Abstract A20.
- (8) Bodanszky, M.; Bodanszky, A. *The Practice of Peptide Synthesis*; Springer Verlag: Berlin, 1984; p 39.

**Table 1.** Crystal Data for FcGlu(OBz)<sub>2</sub> (**2a**), FcCys(SBz)OMe (**2d**), and FcCOOBt (**3**)

	<b>2a</b>	<b>2d</b>	<b>3</b>
empirical formula	C <sub>30</sub> H <sub>29</sub> FeNO <sub>5</sub>	C <sub>22</sub> H <sub>23</sub> FeNO <sub>3</sub> S	C <sub>17</sub> H <sub>13</sub> FeN <sub>3</sub> O <sub>2</sub>
fw	539.4	437.3	347.2
space group	<i>P</i> 2 <sub>1</sub>	<i>P</i> 2 <sub>1</sub> 2 <sub>1</sub>	<i>P</i> 1
<i>a</i> , Å	11.8142(5)	9.957(2)	7.0391(5)
<i>b</i> , Å	9.7560(5)	11.680(2)	10.7922(7)
<i>c</i> , Å	22.9456(10)	36.452(6)	11.1690(7)
α, deg			108.071(5)
β, deg	90.246(5)		107.957(5)
γ, deg			103.896(5)
<i>V</i> , Å <sup>3</sup>	2644.7 (2)	4239.5 (13)	712.5 (2)
<i>Z</i>	2	4	2
ρ <sub>calc</sub> , g/cm <sup>3</sup>	1.355	1.370	1.618
cryst size, mm	0.30 × 0.30 × 0.12	0.30 × 0.08 × 0.05	0.20 × 0.15 × 0.10
μ(Mo Kα), cm <sup>-1</sup>	6.10	6.80	1.07
radiation (monochromated in incident beam)	Mo Kα (λ = 0.710 73 Å), graphite monochromated	Cu (λ = 1.540 60 Å), graphite monochromated	Mo Kα (λ = 0.710 73 Å), graphite monochromated
<i>R</i> , <i>R</i> <sub>w</sub> <sup>a</sup>	0.046, 0.061	0.065, 0.157	0.030, 0.036

$$^a R = \sum(F_o - F_c)/\sum(F_o); R_w = [\sum(w(F_o - F_c)^2)/\sum(wF_o^2)]^{1/2}.$$

(1H, s, H ortho to carboxy group on Cp ring), 4.37 (2H, s, H meta to carboxy group on Cp ring), 4.25 (5H, s, unsubstituted Cp ring), 3.77 (3H, s, -OCH<sub>3</sub>), 1.82 (2H, m, SCH<sub>2</sub>Ph).

**Ferrocenyl-N-Ala(OBz) (2e).** H-Ala-OBzl·Tos (0.70 g, 2.2 mmol) was used. Yield: 0.65 g, 76.6%, yellow microcrystalline solid. MW for C<sub>21</sub>H<sub>21</sub>NO<sub>3</sub>Fe: calc, 391.2; found, 392.1 [M + 1]<sup>+</sup>. <sup>1</sup>H-NMR (δ in ppm, CDCl<sub>3</sub>): 7.37 (5H, m, aromatic H of CH<sub>2</sub>Ph), 6.23 (1H, d, J<sub>NH</sub> = 6.6 Hz, -NH), 5.22 (2H, second-order m, -OCH<sub>2</sub>Ph), 4.80 (1H, m, N(H)CH(R)C(O)), 4.72 (1H, s, H ortho to carboxy group on Cp ring), 4.66 (1H, s, H ortho to carboxy group on Cp ring), 4.36 (2H, s, H meta to carboxy group on Cp ring), 4.21 (5H, s, unsubstituted Cp ring), 1.50 (3H, d, J<sub>HH</sub> = 7.2 Hz, -CH<sub>3</sub>).

**Ferrocenyl-N-Tyr(OBz) (2f).** H-Tyr-OBzl·HCl (0.9 g, 2.2 mmol) was used. Yield: 0.76 g, 72.5%, orange solid. MW for C<sub>27</sub>H<sub>25</sub>NO<sub>3</sub>Fe: calc, 483.3; found, 484.0 [M + 1]<sup>+</sup>. <sup>1</sup>H-NMR (δ in ppm, CDCl<sub>3</sub>): 7.36 (5H, br s, aromatic H of CH<sub>2</sub>Ph), 6.85 (AB quartet of phenolic residue of Tyr), 6.13 (1H, d, J<sub>NH</sub> = 8.0 Hz, -NH), 5.19 (2H, second-order m, -OCH<sub>2</sub>Ph), 5.05 (1H, dm, J<sub>NH</sub> = 7.9 Hz, N(H)-CH(R)C(O)), 4.62 (1H, s, H ortho to carboxy group on Cp ring), 4.57 (1H, s, H ortho to carboxy group on Cp ring), 4.31 (2H, s, H meta to carboxy group on Cp ring), 4.10 (5H, s, unsubstituted Cp ring), 3.10 (2H, t, J<sub>HH</sub> = 6.3 Hz, -CH<sub>2</sub>Ph).

**Ferrocenyl-N-Phe(OBz) (2g).** H-Phe-OBzl·HCl (0.63 g, 2.16 mmol) was used. Yield: 0.88 g, 87.2%, yellow microcrystalline solid. MW for C<sub>27</sub>H<sub>25</sub>NO<sub>3</sub>Fe: calc, 467.3; found, 468.0 [M + 1]<sup>+</sup>. <sup>1</sup>H-NMR (δ in ppm, CDCl<sub>3</sub>): 7.36 (5H, m, aromatic H), 7.30 (2H, m, aromatic H ortho), 7.11 (3H, m, aromatic H meta and para), 6.07 (1H, d, J<sub>NH</sub> = 7.8 Hz, -NH), 5.19 (2H, second-order m, -OCH<sub>2</sub>Ph), 5.04 (1H, dt, J<sub>NH</sub> = 7.6 Hz, J<sub>HH</sub> = 5.5 Hz, -N(H)CH(R)C(O)), 4.62 (1H, s, H ortho to carboxy group on Cp ring), 4.60 (1H, s, H ortho to carboxy group on Cp ring), 4.32 (2H, s, H meta to carboxy group on Cp ring), 4.11 (5H, s, H of unsubstituted Cp ring), 3.19 (2H, dd, J<sub>HH</sub> = 5.9 Hz, J<sub>NH</sub> = 1.9 Hz, -CH<sub>2</sub>Ph adjacent to stereocenter). <sup>13</sup>C-NMR (δ in ppm, CDCl<sub>3</sub>, 20 °C): 171.7 (C=O), 170.0 (C=O), 135.9 (s, quaternary C of Ph), 129.2 (s, Ph), 128.6 (br s, Ph), 127.1 (s, Ph), 124.6 (s, Ph), 120.4 (s, Ph), 73.4 (s, ipso C of Cp), 70.4 (s, 2Cs meta to substituent on Cp), 69.7 (s, unsubstituted Cp ring), 68.2 (s, C ortho to substituent on Cp), 68.0 (s, C ortho to substituent on Cp), 67.2 (s, -OCH<sub>2</sub>Ph), 54.7 (N(H)CH<sub>2</sub>C(O)), 38.0 (s, -CH<sub>2</sub>Ph).

**Ferrocenyl-OBt (3).** Ferrocenecarboxylic acid (0.55 g, 2.4 mmol) was dissolved in CH<sub>2</sub>Cl<sub>2</sub> (10 mL), and solid dicyclohexylcarbodiimide (0.50 g, 2.4 mmol) and HOBT (0.34 g, 2.4 mmol) were added to the stirring solution. After 3 h at room temperature, dicyclohexylurea was removed by filtration. The filtrate was washed with saturated NaHCO<sub>3</sub> solution (50 mL), followed by distilled water (50 mL), and then dried over MgSO<sub>4</sub>. The solvent was removed in vacuo. The crude product (yield 0.79 g, 94.8%) was recrystallized from ethyl acetate and then from diethyl ether to give 0.68 g (81.6%) of dark red crystalline product. The product was recrystallized at -20 °C from EtAc/Et<sub>2</sub>O (1:1) giving dark-red blocks, used in the crystallographic study (*vide infra*). MW for C<sub>17</sub>H<sub>13</sub>N<sub>3</sub>O<sub>2</sub>Fe: calc, 347.2; found, 348.0 [M + 1]<sup>+</sup>. <sup>1</sup>H-NMR (δ

in ppm, CDCl<sub>3</sub>): 7.35–7.32 (4H, m, aromatic H of N<sub>3</sub>C<sub>6</sub>H<sub>4</sub>), 5.21 (2H, s, H ortho to carboxy group on Cp ring), 4.83 (2H, s, H meta to carboxy group on Cp ring), 4.21 (5H, s, unsubstituted Cp ring).

**Structural Studies.** All pertinent crystallographic information is summarized in Table 1.

Crystals of **2a**, **2d**, and **3** were mounted on glass fibers using epoxy resin. Data collection for **2a** and **3** proceeded at -150 °C on a Siemens SMART diffractometer equipped with a CCD detector (Mo Kα). The data for **2a** (**3**) were collected up to a 2θ maximum of 49° (for **3**: 57.5°) using the ω-scan mode. Of 11 939 (for **3**: 8405) reflections measured, 7933 (for **3**: 3644) were unique (7532 with *I* > 2.5σ(*I*)) (for **3**: 3090 with *I* > 2.5σ(*I*)). A total of 256 reflections with 2θ < 49° (for **3**: 92 reflections with 2θ < 57.5°) were missed. An empirical absorption correction was applied. The merging *R* value on significant intensities was 0.019 (for **3**: 0.015). The cell parameters were determined from 8192 (for **3**: 5655) reflections. The refinement was carried out with the NRCVAX<sup>11,12</sup> system of programs. All non-hydrogen atoms were refined anisotropically. The hydrogen atoms were placed in calculated positions and allowed to ride on their parent atoms. Weights based on statistics were used. The refinement (based on *F*<sub>o</sub>) converged to *R* = 0.046, *R*<sub>w</sub> = 0.061 (for **3**: *R* = 0.030, *R*<sub>w</sub> = 0.036).

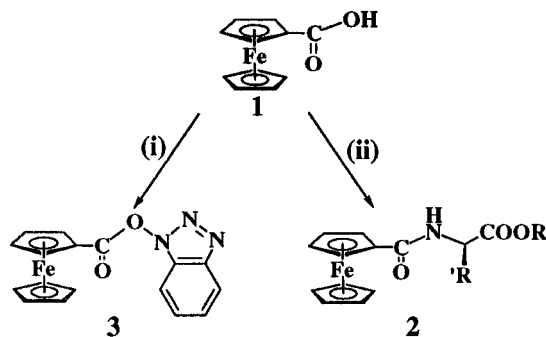
Data collection for **2d** proceeded at room temperature on an ENRAF Nonius CAD 4 diffractometer (Cu Kα). Its unit cell was obtained from 20 carefully centered reflections, obtained by a random search. Monitoring three standard reflections every 100 reflections indicated no decay of the crystal in the X-ray beam. Data were collected at variable scan speeds in the ω-2θ-scan mode in the range of 4.83 < 2θ < 80.00, giving a total of 2121 reflections (1153 with *I* > 2σ(*I*)). The data were corrected for Lorentz and polarization effects. No absorption correction was applied due to the low absorption coefficients (μ = 6.10 (**2a**), 6.80 (**2d**), and 1.07 (**3**)). The structure of **2d** was solved by direct methods and refined by difference Fourier methods using the SHELXTL program package.<sup>9</sup> Hydrogen atoms were introduced at calculated positions. Scattering factors and corrections for anomalous dispersion for all heavy atoms were those of ref 10.

The absolute conformations of **2a** and **2d** were confirmed as a matter of course. For **2a**, the chirality was confirmed using the Rogers method. The Flack method was used for **2d**.

## Results and Discussion

**a. Synthesis of 2a–g and 3.** The reaction of ferrocenecarboxylic acid (**1**) with C-protected amino acid salts under basic conditions in the presence of dicyclohexylcarbodiimide (DCC) and hydroxybenzotriazole (HOBT) cleanly led to the formation

- (9) SHELXTL, Version 5; Siemens Energy & Automation, Inc., 1994.  
 (10) *International Tables for Crystallography*; Kynoch Press: Birmingham, U.K., 1974; Vol. 4.  
 (11) Gabe, E. J.; Le Page, Y.; Charland, J.-P.; Lee, F. L.; White, P. S. J. *Appl. Crystallogr.* **1989**, *22*, 384–387.  
 (12) Le Page, Y.; Gabe, E. J. *J. Appl. Crystallogr.* **1979**, *12*, 464–466.

**Scheme 1.** Synthesis of Ferrocenyl Amino Acid Esters<sup>a</sup>

<sup>a</sup> Key: (i) CH<sub>2</sub>Cl<sub>2</sub>, DCC, HOBT, 3 h; (ii) CH<sub>2</sub>Cl<sub>2</sub>, DCC, HOBT, AA ester (free base), 2 days.

**Table 2.** Selected <sup>1</sup>H-NMR Spectroscopic Data for the Ferrocenyl Amino Acid Esters **2a–g** (CDCl<sub>3</sub>, δ in ppm, Room Temperature)

compd	NH	CH	Cp <sup>ortho</sup>	Cp <sup>meta</sup>	Cp
<b>2a</b>	6.63 (d, 7.7)	4.77	4.77, 4.64	4.34	4.21
<b>2b</b>	6.22 (s)	4.15	4.72	4.36	4.28
<b>2c</b>		4.70	4.86, 4.70	4.36	4.24
<b>2d</b>	6.47 (d, 7.0)	4.94	4.73, 4.61	4.37	4.25
<b>2e</b>	6.23 (d, 6.6)	4.80	4.72, 4.66	4.36	4.21
<b>2f</b>	6.13 (d, 8.0)	5.05	4.62, 4.57	4.31	4.10
<b>2g</b>	6.07 (d, 7.8)	5.04	4.62, 4.60	4.32	4.11

of orange to yellow coupling products Fc-AA (**2**) (AA = Glu(OBz)<sub>2</sub> (**2a**), Gly(OEt) (**2b**), Pro(OBz) (**2c**), Cys(SBz)OMe (**2d**), Ala(OBz) (**2e**), Tyr(OBz) (**2f**), Phe(OBz) (**2g**)) (Scheme 1).

This reaction is related to that used by Heller to incorporate ferrocene moieties into proteins.<sup>6a,b</sup> Very recently, a ferrocene moiety was incorporated into the lysine side chain and the product characterized by spectroscopic methods.<sup>13</sup> The product can be easily separated from organic byproducts (e.g., dicyclohexylurea) and excess reagents (e.g., hydroxybenzotriazole and unreacted starting materials) by filtration and washings with aqueous saturated KHCO<sub>3</sub> solution and 5% citric acid. All ferrocenyl amino acid esters are diethyl ether soluble and were recrystallized from diethyl ether to give crystalline compounds (**2a–b**, **2d–g**). **2c** is a viscous oil.

In the absence of C-protected amino acids, the ferrocenyl benzotriazole ester (**3**) was obtained as a dark red crystalline material, which is air and moisture stable in common solvents. This compound does not hydrolyze under aqueous extraction conditions employed in the isolation and purification of ferrocenyl amino acid ester (aqueous saturated KHCO<sub>3</sub>, 5% citric acid). In the presence of amino acids (free base), **3** reacts as expected by amidation to give the ferrocenyl amides.

**b. Identification of Compounds 2a–g and 3.** All compounds were fully characterized by a combination of electrospray-MS (**2a–g**, **3**), NMR spectroscopies, (**2a–g**, **3**), and X-ray crystallography (**2a**, **2d**, and **3**; *vide infra*). Electrospray-MS, a very soft ionization method widely used for biological molecules, confirmed the molecular weight of all the compounds described. Table 2 summarizes selected <sup>1</sup>H-NMR spectroscopic data for **2a–g**. All spectra were fully assigned using DEPT and 2D-COSY techniques.

The presence of the chiral carbon center in the amino acid part of the molecule effectively generates two diastereotopic sides of the molecules. This renders the two H atoms adjacent to the amide functionality on the Cp ring magnetically non-equivalent, giving rise to two singlets in narrowly defined

**Table 3.** Selected Bond Distances (Å) and Angles (deg) for **2a**

molecule 1		molecule 2	
(a) Bond Distances			
av Fe(1)–C	2.041(5) (for CpR)	av Fe(101)–C	2.022(7)
av Fe(1)–C	2.047(5) (for Cp)	av Fe(101)–C	2.065(9)
O(1)–C(11)	1.226(6)	O(101)–C(111)	1.222(6)
C(1)–C(11)	1.499(7)	C(101)–C(111)	1.507(7)
C(11)–N(1)	1.347(6)	C(111)–N(101)	1.342(7)
(b) Bond Angles			
O(1)–C(11)–N(1)	122.5(4)	O(101)–C(111)–N(101)	122.8(5)

regions (δ 4.86–4.62 and 4.57–4.70). The two diastereotopic H atoms in *meta* positions with respect to the amide group on the Cp ring appear as a slightly broadened singlet (5–8 Hz) in the shift range of δ 4.31–4.37. The H atoms of the unsubstituted Cp ring are observed as singlets for all compounds. The H atom of the amide NH is observed as a doublet due to coupling with the adjacent chiral CH group, with coupling constants ranging from 8.0 Hz (for **2f**) to 6.6 (for **2e**).

<sup>13</sup>C-NMR spectroscopy is a sensitive tool to qualitatively evaluate changes in electron density caused by substituent influences of the different amino acids.<sup>14</sup> Interestingly, the measurements show that the shift of the Cp C atom carrying the amide substituent is almost invariant with respect to amino acid substitution (between δ 75 and 73). Hence, the <sup>13</sup>C-NMR results seem to suggest that no significant substituent influence exists. Likewise the signal due to the ortho and meta C atoms of the substituted Cp ring and those of the unsubstituted Cp ring exhibit signals which do not vary significantly from one amino acid to another.

The cyclic voltammograms for **2a–d** were measured in acetonitrile solution, with ferrocene as an internal redox standard. As expected, **2a–d** exhibit fully reversible one-electron oxidations, attributed to a ferrocene-based oxidation, resulting in the formation of a ferrocenium cation. There are some slight variations in oxidation potential, with respect to the attached amino acid. The half-wave potential of **2c** (172 mV vs Fc/Fc<sup>+</sup>) is lower than those of **2a** (180 mV vs Fc/Fc<sup>+</sup>), **2b** (181 mV vs Fc/Fc<sup>+</sup>), and **2d** (191 mV vs Fc/Fc<sup>+</sup>). Currently, we are investigating the redox properties in more detail and hope to be able to correlate them to the electronic structures of the compounds.

**c. Structural Studies.** Selected bond distances and angles for **2a** are given in Table 3. An ORTEP view of one of the molecules of complex **2a** is given in Figure 1. **2a** crystallizes in the monoclinic space group *P*2<sub>1</sub> with two independent molecules per asymmetric unit. In each molecule, the Cp rings are virtually parallel to each other (Cp–Fe–Cp angles: 2.1–(3)° (for molecule 1) and 1.6(4)° (for molecule 2)). The distances of Fe to the C atoms of the Cp rings was normal and compare well with those of other ferrocene structures.<sup>15</sup> Interestingly, the Cp internal C–C bond distances in the substituted Cp rings (1.430(9) and 1.424(12) Å) are longer than in the unsubstituted Cp ring (1.411(12) and 1.404(15) Å) for

(14) (a) van de Kuil, L. A.; Luitges, H.; Grove, D. M.; Zwicker, J. W.; van der Linden, J. G. M.; Roelofsen, A. M.; Jenneskens, L. W.; Drenth, W.; van Koten, G. *Organometallics* **1994**, *13*, 468. (b) Weisman, A.; Gozin, M.; Kraatz, H.-B.; Milstein, D. *Inorg. Chem.* **1996**, *35*, 1792–1797.

(15) (a) Grossel, M. C.; Goldspink, M. R.; Hrijac, J. A.; Weston, S. C. *Organometallics* **1991**, *10*, 851–860. (b) Hall, D. C.; Danks, I. P.; Nyburg, S. C.; Parkins, A. W.; Sharpe, N. W. *Organometallics* **1990**, *9*, 1602–1607. (c) Wang, J.-T.; Yuan, Y.-F.; Xu, Y.-M.; Zhang, Y.-W.; Wang, R.-J.; Wang, H.-G. *J. Organomet. Chem.* **1994**, *481*, 211–216. (d) Seidelmann, O.; Beyer, L.; Richter, R. Z. *Naturforsch.* **1995**, *50B*, 1679–1684. (e) Seidelmann, O.; Beyer, L.; Zdobinsky, G.; Kirmse, R.; Dietze, F.; Richter, R. Z. *Anorg. Allg. Chem.* **1996**, *622*, 692–700. (f) Wen, Z.; Li, F.-Z.; Liu, Q.-W.; Huang, X.-Y. *Jiegou Hauxue* **1995**, *14*, 108–112.

(13) McCafferty, D. G.; Bishop, B. M.; Wall, C. G.; Hughes, S. G.; Mecklenburg, S. L.; Meyer, T. J.; Eickson, B. W. *Tetrahedron* **1995**, *51*, 1093–1106.

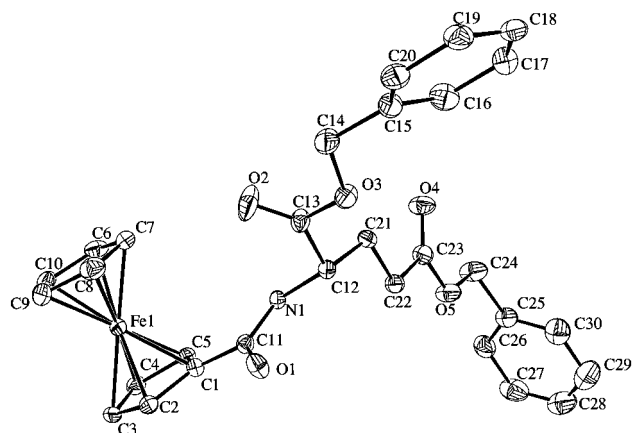


**Figure 1.** ORTEP plot of **2a** (30% probability level) showing the adopted numbering scheme. The second molecule has similar structural features (see Supporting Information). Hydrogen atoms are omitted for clarity.

both molecules. This has been documented before.<sup>15</sup> The distances of the carbonyl carbon to the Cp ring (C(1)–C(11) 1.499(7) Å and C(101)–C(111) 1.507(7) Å) are normal C–C single bond distances. It is interesting to note that nonstrained ferrocenyl amides have C–C(Cp) bonds ranging from 1.471(4) to 1.477(7) Å. However, for the macrocyclic 1,1'-[1,4,10,13-tetraoxa-7,16-diazacyclooctadecane-7,16-diyl]dicarbonylferrocene, a long C–C(Cp) bond of 1.501(7) Å has been observed.<sup>15a</sup> This and other distortions in that particular structure have been attributed to minimizations of ring strain in the macrocyclic part of the molecule, rather than to specific intramolecular interactions. The amide C(O)–N group is planar in both molecules. The carbonyl C–O distances compare well with those of other ferrocenyl amides. The amide C–N distances (C(11)–N(1) 1.347(6) Å and C(111)–N(101) 1.342(7) Å) exhibit significant single-bond character. The amide plane is rotated out of the Cp ring plane by 14.1(2)° (for molecule 1) and 18.4(3)° (for molecule 2).

The nonbonding distances between the carbonyl group and an amide NH of an adjacent molecule are about 2.8 Å (O(1)···N(101) 2.81 Å and O(101)···N(1) 2.80 Å), indicating the presence of strong H-bonding between neighboring molecules in the solid state. The IR spectrum shows a very broad band at 3400 cm<sup>-1</sup> assigned to  $\nu(\text{N–H})$ , confirming H-bonding. Analysis of the unit cell reveals a linear chainlike structure of molecules linking through NH···O=C hydrogen bonding. NH to water oxygen<sup>16</sup> and NH···O=C<sup>16b,17</sup> are well documented in the literature.

Figure 2 shows an ORTEP drawing of **2d**. Pertinent bond distances and angles are summarized in Table 4. **2d** crystallizes in the orthorhombic space group  $P2_12_12_1$  with two independent molecules per asymmetric unit. The structural features are very similar to those of **2a**, with both molecules having parallel Cp rings (Cp–Fe–Cp: molecule 1, 1.83°; molecule 2, 1.52°). The amide group is slightly rotated out of the plane of the Cp ring to which it is linked (molecule 1, 5.44°; molecule 2, 11.95°). The S–C distances (range 1.77(2)–1.823(6) Å) and the C–S–C angle of 102.1(7)° are normal for thioether linkages.<sup>18</sup> The individual molecules are linked by N–H···O=C bonding; N···O

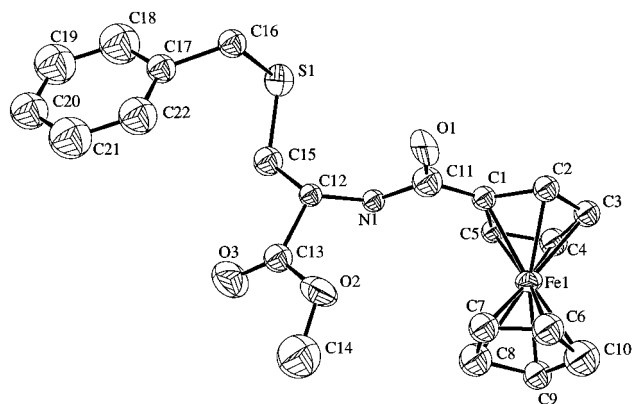


**Figure 2.** ORTEP drawing of **2d** (30% probability level). Only one of the molecules of the asymmetric unit is shown here. Hydrogen atoms are omitted for clarity.

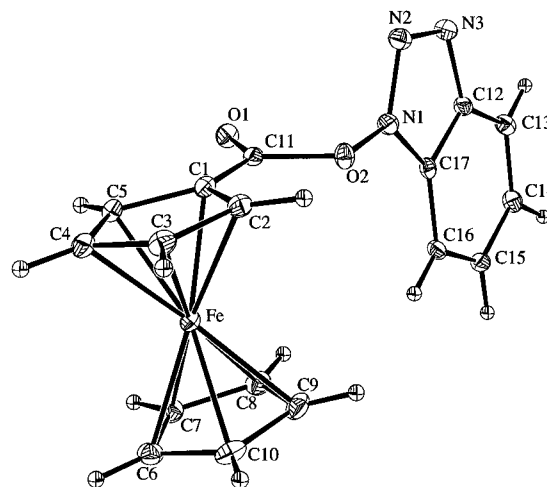


**Figure 3.** ORTEP drawing of **3** (30% probability level).

**Table 4.** Selected Bond Distances (Å) and Angles (deg) for **2d**

molecule 1		molecule 2	
(a) Bond Distances			
av Fe(1)–C	2.03(2) (for CpR)	av Fe(101)–C	2.02(2)
av Fe(1)–C	2.04(2) (for Cp)	av Fe(101)–C	2.07(3)
O(1)–C(11)	1.21(2)	O(101)–C(111)	1.27(2)
C(1)–C(11)	1.43(2)	C(101)–C(111)	1.48(2)
C(11)–N(1)	1.34(2)	C(111)–N(101)	1.39(2)
S(1)–C(15)	1.77(2)	S(1)–C(15)	1.79(2)
S(1)–C(16)	1.823(6)	S(1)–C(16)	1.80(1)
(b) Bond Angles			
O(1)–C(11)–N(1)	123.6(26)	O(101)–C(111)–N(101)	119.3(30)
C(15)–S(1)–C(16)	102.1(7)	C(115)–S(101)–C(116)	102.2(7)

**Table 5.** Selected Bond Distances (Å) and Angles (deg) for **3**

(a) Bond Distances			
av Fe(1)–C	2.050(2) (for CpR)	av Fe(1)–C	2.053(2) (for Cp)
O(1)–C(11)	1.196(2)	C(1)–C(11)	1.450(3)
C(11)–O(2)	1.427(2)		
(b) Bond Angle			
O(1)–C(11)–O(2)	121.3(2)		

2.84 Å), forming endless chains similar to those observed in **2a** and other amino acid structures.<sup>16b,17c</sup>

The crystal structure of **3** is shown in Figure 3. Selected bond distances and angles are given in Table 5. **3** crystallizes in the triclinic space group  $P\bar{1}$ . The ferrocene moiety is in the eclipsed conformation with the ester group being slightly rotated out of the plane of the Cp ring to which it is attached (10.06(10)°). The dimensions within the ferrocene moiety are normal.<sup>15</sup> Interestingly, the benzotriazole (Bt) substituent is

(16) (a) Freeman, H. C.; Taylor, M. R. *Acta Crystallogr.* **1965**, *18*, 939–952. (b) Freeman, H. C.; Robinson, G.; Schoone, J. C. *Acta Crystallogr.* **1964**, *17*, 719–730.

(17) (a) Marsh, R. E.; Glusker, J. P. *Acta Crystallogr.* **1961**, *14*, 1110–1116. (b) Leung, Y. C.; Marsh, R. E. *Acta Crystallogr.* **1958**, *11*, 17–31. (c) Haas, D. J. *Acta Crystallogr.* **1965**, *19*, 860–861.

(18) (a) *Handbook of Chemistry and Physics*, 67th ed.; CRC Press, Inc.: Boca Raton, FL, 1987; pp F160–F162. (b) Boorman, P. M.; Gao, X.; Parvez, J. *Chem. Soc., Chem. Commun.* **1992**, 1656–1658.

rotated out of the ester plane by  $96.56(6)^\circ$ , allowing no efficient interaction between the  $\pi$ -systems of the Cp ring and the benzotriazole. A similar behavior has been observed for benzoylferrocene,<sup>19</sup> where the solid state structure shows the phenyl ring rotated out of the Cp plane by  $40.4^\circ$ . Steric interference does not allow coplanarity of the Cp and Ph groups.<sup>19</sup> Similar steric problems are most likely responsible for the arrangement of the Bt substituent.

The C(11)–O(1) bond distance of  $1.196(2) \text{ \AA}$  is significantly shorter than those observed for ferrocenecarboxylic acid<sup>20</sup> ( $1.261(15) \text{ \AA}$ ) and ferrocenedicarboxylic acid ( $1.228(3) \text{ \AA}$ ).<sup>21</sup> It is also shorter than those of other ferrocenecarboxylic esters, such as 2-(1-hydroxyethyl)-1-ferrocenecarboxylic acid methyl ester (C=O  $1.205(4) \text{ \AA}$ )<sup>22</sup> and 3-(diphenylphosphino)-1-ferrocenecarboxylic acid methyl ester (C=O  $1.204(3) \text{ \AA}$ ).<sup>23</sup> The C(11)–O(2) bond distance is about  $0.09 \text{ \AA}$  longer than those of other esters ( $1.427(2) \text{ \AA}$ ). This crystallographic information fits well with the observed facile amidation of active esters in the presence of primary and secondary amines. Being a long ester bond, it is inherently weak and reactive and hence it will rapidly react to form an amide bond.

(19) Butler, I. R.; Cullen, W. R.; Rettig, S. J.; Trotter, J. *Acta Crystallogr.* **1988**, *C44*, 1666–1667.

(20) Cotton, F. A.; Reid, A. H., Jr. *Acta Crystallogr.* **1985**, *C41*, 686–688.

(21) Palenik, G. J. *Inorg. Chem.* **1969**, *8*, 2744–2749.

(22) Luo, Y.; Barton, R. J.; Robertson, B. E. *Acta Crystallogr.* **1990**, *C46*, 1388–1391.

(23) Podlaha, J.; Stepnicka, P.; Ludvik, J.; Cisarova, I. *Organometallics* **1996**, *15*, 543–550.

## Summary and Outlook

Our studies described the facile synthesis and characterization of novel ferrocenoyl amino acid esters. While  $^{13}\text{C}$ -NMR spectroscopy does not provide any insight into the electron density variation presumably caused by a variation of the amino acid, CV measurements suggest that there is an influence. We are currently investigating this in more detail. We are in the process of carrying out high-level calculations based on density functional theory to gain further insight into the electronic structures of the complexes. This may allow us to rationalize the changes in redox potential. Initial results show that it is possible to carry out solution peptide syntheses using ferrocenoyl amino acid esters, by a deprotection–coupling sequence. We are planning a full structural (solution and solid state) characterization of all products to properly evaluate structural changes.

**Acknowledgment.** We wish to express our gratitude to Abdelaziz Houmam for electrochemical measurements. The NRC Biological Institute generously provided access to its NMR and mass spectroscopic facilities. H.-B.K. is the recipient of an NRC research associateship (1996–1998).

**Supporting Information Available:** Structural reports, unit cell and ORTEP diagrams, and tables of isotropic and anisotropic displacement parameters, atomic positional parameters for H and non-H atoms, and bond lengths and angles for **2a**, **2d**, and **3** (29 pages). Ordering information is given on any current masthead page.

IC961454T